Available online at www.sciencedirect.com
SCIENCE DIRECT®
Journal of Membrane Science 226 (2003) 101–110
journal of MEMBRANE SCIENCE
www.elsevier.com/locate/memsci

Dynamic desorption of adsorbing species under cross membrane pressure difference: a new defect characterisation approach in zeolite membranes

Olga Pachtová[1], Izumi Kumakiri, Milan Kočiřik[1], Sylvain Miachon, Jean-Alain Dalmon*

Institut de Recherches sur la Catalyse, Centre National de la Recherche Scientifique, 2 Av. A. Einstein, 69626 Villeurbanne Cedex, France

Received 17 February 2003; received in revised form 7 July 2003; accepted 7 July 2003

Abstract

Alumina–zeolite composite membranes were prepared on alumina porous tubular supports by single-step in situ hydrothermal synthesis. Hydrogen/*n*-butane separation factor was used as a criterion to evaluate the presence of defects. Five membranes of different qualities were selected. The hydrogen permeance through the membranes, plugged beforehand with two strongly adsorbing gases (water and *n*-butane), was followed with time at room temperature. The dynamic desorption thus observed was correlated to the quality of the membrane.

Keywords: Zeolite membrane; Membrane defect; Desorption; Water; *n*-Butane

1. Introduction

Making zeolite membranes able to separate gas molecules has been a goal of many authors in the last two decades. Zeolite membranes usually have a polycrystalline structure. Permeating molecules can pass through both zeolite pores (intracrystalline pathways) and gaps between crystals (membrane defects or inter-crystalline pathways) [1]. The last decade has seen a major breakthrough in the synthesis of high quality zeolite membranes with potential for industrial gas separation and pervaporation applications [2–12]. The separation properties of the membrane are determined by the presence of defects, their adsorption characteristics, and the gas properties in the mixture (kinetic diameter, adsorption strength and diffusivity). Therefore, gas mixture separation through the membrane can be used as a method for evaluation of the membrane quality [13–18]. Nevertheless, the characterisation of gas mixtures crossing the membrane necessitates sophisticated equipment. This technique is therefore difficult to apply to industrial production and quality control. The permporometry technique, as described by Nakao [19] has been tentatively used on microporous membranes by Tsuru et al. [20]. In this case, the concentration of an adsorbing gas is kept constant with time on both sides of the membrane, and the permeation of a non-adsorbing gas is followed. The present paper presents different but more

* Corresponding author. Tel.: +33-4-7244-5368; fax: +33-4-7244-5399.
E-mail address: dalmon@catalyse.univ-lyon1.fr (J.-A. Dalmon).
[1] On leave from the J. Heyrovský Institute of Physical Chemistry, Academy of Sciences of the Czech Republic, Dolejskova 3, 18223 Praha 8, Czech Republic.

0376-7388/$ – see front matter © 2003 Elsevier B.V. All rights reserved.
doi:10.1016/j.memsci.2003.07.017

simple approach, the dynamic desorption of a gas adsorbed beforehand (water or *n*-butane), under pressure difference of a non-adsorbing gas (hydrogen).

2. Experimental

2.1. Material

ZSM-5 membranes were prepared by growing zeolite crystals into the pores of a multilayer α-alumina membrane supports, as described elsewhere [4,21]. They were tubes of 15 cm length, 6.5 mm inner diameter, provided by the Société des Céramiques Techniques (now PALL-Exekia), type T1-70. The support consisted of three layers. The first layer was made of 10-μm pores, for a thickness of 1.5 mm. Two layers of smaller pore size, 0.64 and 0.2 μm, with a respective thickness of about 40 and 20 μm, are located on top of the first layer. The support tubes were equipped with 1-cm enamel endings for proper sealing on graphite rings. A precursor 120 g/l (2 mol/l) Degussa Aerosil 380 silica solution in 0.9 mol/l tetrapropyl ammonium hydroxide (TPAOH, diluted Aldrich: 25,453-3) was matured under magnetic stirring for 72 h and centrifuged to eliminate any particle left in suspension. The molar ratio of the silica, TPAOH and water in the precursor was 2:0.9:55.6. The support tube was then immersed into the solution in a Teflon insert placed in a stainless steel autoclave. The autoclave was heated for about 90 h up to 443 K. Before calcinations, the membrane was checked for gas tightness.

The membrane was then calcined at 500 °C in a mixture of 5% O_2 and 95% N_2 with a flow rate of 20 ml/min (1.7 °C/min heating rate), until the hydrogen permeance reached a plateau (6 h).

To avoid potential effects of sealing on the membrane permeance measurement, all operations with the membranes (pre-treatment, adsorption, separation test, desorption) were carried out inside the same module, while the tube membrane kept mounted in during the whole set of experiments.

2.2. Experimental set-up

A stainless steel flow system was used for all experiments (pre-treatment, separation tests, H_2 permeation, adsorption and desorption) (see Fig. 1). All transport measurements were carried out at room temperature.

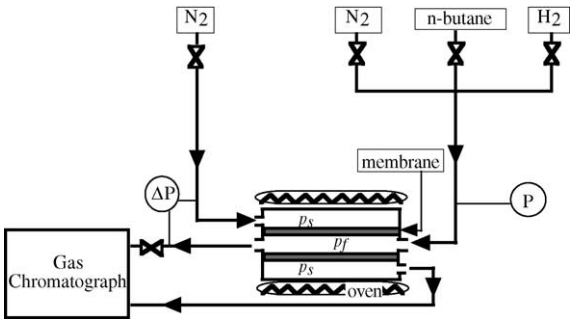

Fig. 1. Schematics of the membrane set-up, shown as an example for the gas separation configuration: pressure difference $p_f - p_s = \Delta p \approx 0$, p_f is the pressure in the feed (tube) side and p_s the pressure in the sweep (shell) side of the membrane. Please note the pressure (p) & pressure difference (Δp) sensors as well as the gas chromatograph analyzer (TCD/FID, necessary only for gas separation experiments).

2.3. Pre-treatment

A high temperature pre-treatment (HTP) was used to remove any adsorbed gases from a previous test or moisture possibly adsorbed from air. The membranes were heated at a rate of 1 °C/min up to 400 °C and kept at this temperature for 6 h. This pre-treatment was carried out in nitrogen stream flowing along both tube and shell sides of the tubular membrane at a rate of 20 ml/min. Well reproducible values of hydrogen permeance through the membrane at room temperature after HTP were obtained. This value is noted here '$\prod_{H_2(max)}$' and hereafter referred to as the 'maximal hydrogen permeance'. To determine the correct temperature used during this step, the following procedure was followed. A set of experiments was carried out by controlling hydrogen permeance after treatments at different temperature. After water adsorption, a temperature as high as 180 °C was necessary to reach the maximum hydrogen permeance. After hydrocarbon adsorption, a temperature of 360 °C was necessary. As a consequence, 400 °C was used to keep a safe margin.

2.4. Butane/hydrogen separation factor

Separation tests were carried out in the set-up configured as shown in Fig. 1. The gas mixture was fed

on the tube side of the membrane, while nitrogen was used as a counter-current sweep gas, in order to remove the permeated components from the shell side. The measurements were carried out from an equimolar mixture of hydrogen and *n*-butane diluted in nitrogen (N_2 flow rate: 55 ml/min, H_2: 11 ml/min, *n*-butane: 11 ml/min) with pressures close to 100 kPa on both sides of the membrane. The sweep flow rate was set-up at 52 ml/min. The separation factor was calculated from steady state data, which were obtained after 60 min, from the following expression:

$$\mathrm{Sf} = \frac{x_{\mathrm{H_2}} y_{n\text{-butane}}}{y_{\mathrm{H_2}} x_{n\text{-butane}}}$$

where x and y are the molar fraction of hydrogen or *n*-butane in the feed and sweep gas, respectively.

The membrane separation ability for a mixture of adsorbing and non-adsorbing gases at low temperature is based on adsorption. The adsorption of the stronger adsorbing species (butane in this case), in the zeolite pores, hinders hydrogen permeation. The presence of even a small number of defects would ruin such a process, due to the high non-separative transfer in larger pores. Considering this separation mechanism, the butane/hydrogen separation factor is taken as relevant a quality indicator.

2.5. Hydrogen single gas permeation

The hydrogen single gas permeation, denoted hereafter as '$\prod_{H_2}$', was carried out at a 100-kPa pressure drop across the membrane at room temperature, in dead-end mode. The gas used was >99.9 pure from the cylinder, and further purified through two adsorption cartridges (adequate for hydrocarbons and water) upstream from the membrane. The pressure on the permeate side was kept at 101 kPa. The effective membrane area was 0.0028 m^2.

2.6. Water adsorption in the membrane

Two saturators were placed prior to the module. They allowed adsorption of water vapour into the membrane using a wet nitrogen stream on both sides. Two relative pressures of water were used: 0.15 and 0.65, i.e. 0.35 and 1.5 kPa water partial pressure, respectively. They were obtained by mixing dry and saturated nitrogen. The water relative pressure at the outlet was monitored by an absolute humidity-meter (Hygrocor Coreci). The pressure difference across the membrane was kept nil. When the water concentration at the outlet reached the water concentration at the inlet of the membrane, it was considered saturated. This was usually achieved after 4–5 h. The inlet water concentration was checked using the humidity-meter before starting the membrane saturation process. The average amount of water adsorbed in the membranes was 8–9 mg for a relative pressure in the feed stream of 0.16, and 20–30 mg for 0.65, as calculated by integrating the outlet gas humidity.

2.7. n-Butane adsorption in the membrane

The adsorption of *n*-butane was actually obtained after the *n*-butane/hydrogen separation test. The duration of the test was 60 min and the partial pressure of *n*-butane 14 kPa. Based on *n*-butane adsorption isotherms in ZSM-5 measured by Vlugt [22] and Sun et al. [23] the butane load under 14 kPa pressure at 298 K corresponds to 8–10 molecules per unit cell.

2.8. Desorption

Desorption of water or *n*-butane was carried out under the conditions of hydrogen single gas permeation measurements (i.e. under a pressure difference of 100 kPa across the membrane). The desorption was followed by monitoring the hydrogen permeance through the membrane.

3. Results

3.1. Separation factors

After *n*-butane/hydrogen separation testing, five membrane samples with various qualities were selected. Table 1 shows the selected membranes and their hydrogen permeance $\prod_{H_2}$ after high temperature pre-treatment. The values of separation factor 130 and 27 indicate membranes with much fewer defects than in samples with values of 10, 6 and 4.

3.2. Water desorption

After 18 h of 100-kPa tube-side hydrogen overpressure, the hydrogen permeance of all tested membranes

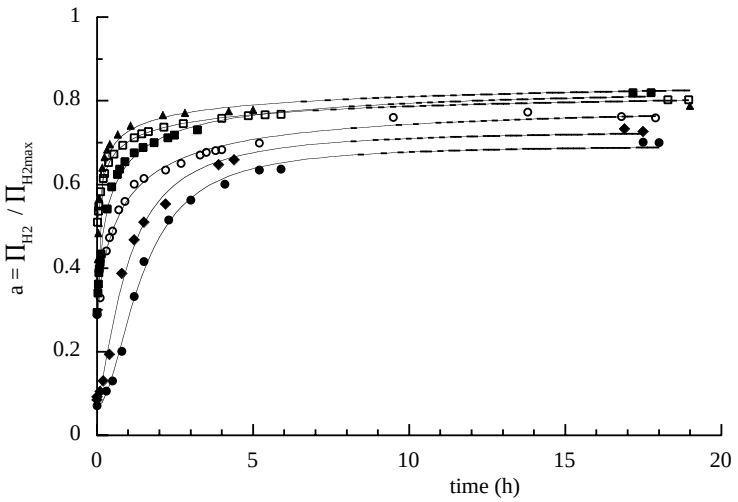

Fig. 2. Water desorption from the membranes A, B, E as followed by the evolution of hydrogen permeance through the membrane: (□/■) membrane A; (●, ◆/○) membrane B; (▲) membrane E. The membranes were wetted at $p_{rel} = 0.15$ (open marks) and 0.65 (solid marks). Note that the actual first value is taken at $t < 1$ mn, but not strictly 0 for technical reasons. Therefore, this value should not be taken too precisely.

reached 70–80% of their original value $\prod_{H_2(max)}$ (cf. Fig. 2).

3.3. *n*-Butane desorption

The hydrogen permeance evolved relatively quickly through the lower quality membranes (C, D, E) and reached 85–90% of the original value, $\prod_{H_2(max)}$, after approximately 10 h (see Fig. 3). A dramatically different situation occurred during *n*-butane desorption from the higher quality membrane B. Even after 23 h the hydrogen permeance kept at very low values. This experiment was repeated on a shorter time scale on the membrane A with similar results. That indicates that *n*-butane molecules could not desorb from the membrane passing through pores in this case.

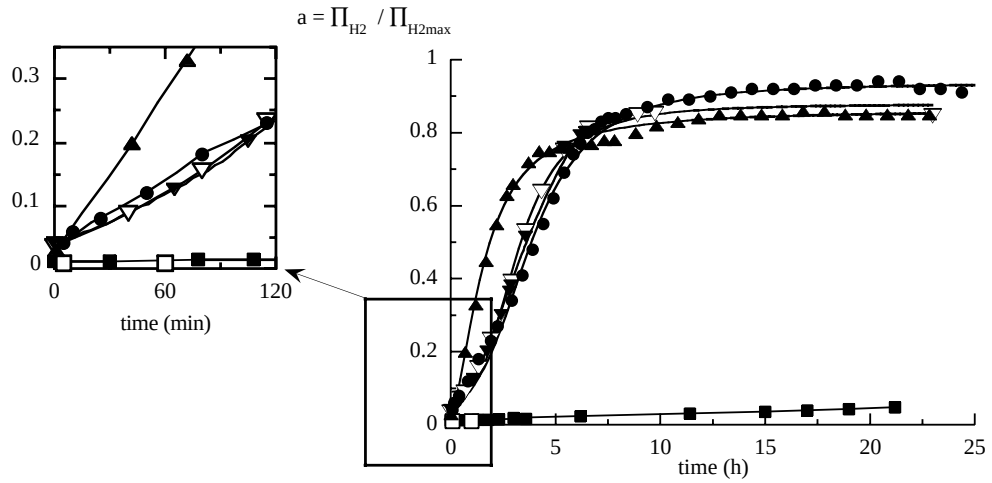

Fig. 3. Desorption curves of *n*-butane from the membranes saturated at 14 kPa *n*-butane partial pressure: (□/■) membrane B; (▲) membrane C; (●) membrane D; (▼/▽) membrane E; open marks show a reproduction of the experiment.

Table 1
Membrane samples used and their characteristics obtained after high temperature pre-treatment

Membrane sample	H_2/*n*-butane separation factor, Sf at room temperature	$\prod_{H_2(max)}$ (10^{-7} mol/m^2 s Pa) at room temperature
A	130	5
B	27	4
C	10	5
D	6	15
E	4	15

4. Discussion

4.1. Critical diameter for adsorption in the membrane

During the adsorption step, the membrane is submitted to a certain partial pressure of an adsorbing gas (i.e. water and butane here). A first approach could be to consider that the different types of pores are filled up, and therefore plugged for all sizes up to a certain "critical diameter".

This adsorption step can be compared to the adsorption isotherms of different materials. For example, *n*-butane completely fills the channel pores of MFI zeolite (channel size 0.51–0.56 nm), at relatively low relative pressure, as shown in Fig. 4.

On the same figure, it can be noted that the zeolite L, with a larger 0.78 nm pore size is also saturated under a 14-kPa pressure of butane, whereas MCM-41, with a pore size of 3 nm is not saturated. Even if the material surface properties are different, it may be assumed that in the case of this work, the only pores remaining open after the adsorption step are inter-crystalline pores. A first conclusion could be that the pore critical diameter, for a butane pressure of 14 kPa, is located between 0.78 and 3 nm. The mechanism of water adsorption should be similar. However, in this case, all the membranes tested behave similarly. This point will be addressed later.

Another approach to the evaluation of the critical diameter could be to use Kelvin equation for capillary condensation. As noted by Nakao [19] and Tsuru et al. [20], the condensation pore radius should then be increased by the thickness of an adsorption layer (0.5 nm for butane, approximately). In this case, one can obtain the following Table 2.

One also needs to take into account the approximation of Kelvin equation, originally designed for an infinite length capillary, and not a porous network. It may be concluded once again that the critical diameter for butane in the conditions of this work is larger that the MFI zeolite channel size.

Therefore, it can be thought that the pore-plugging process occurring during the adsorption step is due to a combined adsorption in zeolite pores and condensation in other pores smaller than the critical diameter.

4.2. Butane desorption

The phenomenon of *n*-butane desorption will be discussed qualitatively. If any, defects larger than the critical diameter are not plugged during the adsorption

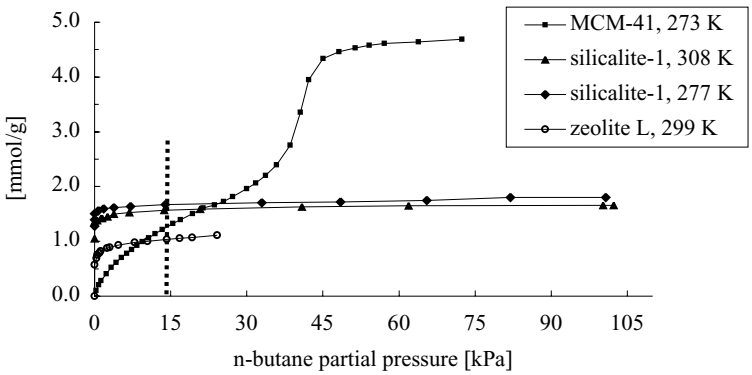

Fig. 4. Adsorption isotherms of *n*-butane in zeolites with various channel size: MCM-41, 3 nm [24]; zeolite L, 0.78 nm [25]; silicalite, 0.51–0.56 nm [23]. Please note the dashed line marking the 14-kPa butane partial pressure used during this work.

Table 2
Kelvin capillary condensation diameter for the conditions used in this work (taken as critical diameter)

	n-Butane at relative pressure 6% (i.e. 14 kPa, T_{room})	Water at relative pressure 15%	Water at relative pressure 65%
Capillary condensation diameter (nm)	1.7	11	49

process. Therefore, hydrogen starts to permeate through these open large pores in the separative layer. This starting hydrogen permeation is followed by a significant increase with time. This can be explained by the desorption of *n*-butane from the rest of the membrane pores (zeolite channels and inter-crystalline pores smaller than the critical diameter) into the passageways resulting from the defects, as *n*-butane concentration in these passageways is permanently and significantly diminished by the hydrogen stream.

On the other hand, hydrogen permeance through the high quality membranes remained very low. It seems that high quality membranes only contain ZSM-5 micropores and maybe narrow inter-crystalline channels of a size not larger than the critical diameter. Therefore, no open pores are present to allow the start of the desorption process described earlier. Then, the hydrogen permeance through the saturated membrane could only be due to a free desorption process, which is obviously very slow, as shown in Fig. 3.

We also considered a possibility of oligomerisation of possible organic impurities. The low-temperature oligomerisation of small olefins on ZSM-5 zeolites was suggested by Berg and co-workers [26–28] and Zikanova et al. [29]. We used a *n*-butane cylinder with the following impurities content: isobutane: 150 ppm; C3 (C_3H_8 and C_3H_6): 30 ppm; other unsaturated <50 ppm. This possibility of oligomerisation was ruled out when it was demonstrated that ammonia molecules would move out *n*-butane molecules (adsorbed from the same cylinder [30]). The fact that oligomers could be easily shifted by ammonia molecules at room temperature seems very unlikely.

4.3. Water desorption

On the opposite of what had been presented for butane desorption, no practical differences were observed for water desorption between lower and higher quality membranes, in spite of the high adsorption and condensation ability of water. As mentioned in Fig. 2, care should be taken regarding the first point measured just after the start of the desorption process. The time needed to establish hydrogen overpressure and the duration of the flux measurement are large when compared to water desorption speed. Nevertheless, water desorption from membrane B (separation factor 27, hydrogen permeance 0.5 μmol/m^2 s Pa) is repeatedly slower than from membrane A (Sf = 130, $\prod_{H_2(max)} = 0.4\,\mu mol/m^2 s\,Pa$). This may be due to some differences in the membrane structure. For example, the lower hydrogen permeance may reflect a higher effective thickness, that may slower the desorption process.

A water diffusion coefficient, two orders of magnitude higher than for *n*-butane in MFI channel systems, could explain the unexpected difference between water and butane desorption, as shown in Table 3.

The kinetic effect of different desorption rates of water and *n*-butane molecules is well perceptible already on the lower quality membrane E (see Fig. 5). Whereas water desorbed already after 2 h, *n*-butane needed more than 8 h.

Table 3
Diffusion coefficients of water and *n*-butane in MFI channel system at low loading

	T (K)	Si/Al ratio	*D* (m^2/s)	Reference
Water	298	Silicalite	3.3×10^{-9}	[31]
	298	25	5×10^{-9}	[32]
n-Butane	298	Silicalite	Straight channel: 8.7×10^{-11}; sinusoidal channel: 1.5×10^{-11}	[33]
	298	53	11×10^{-11}	[34]

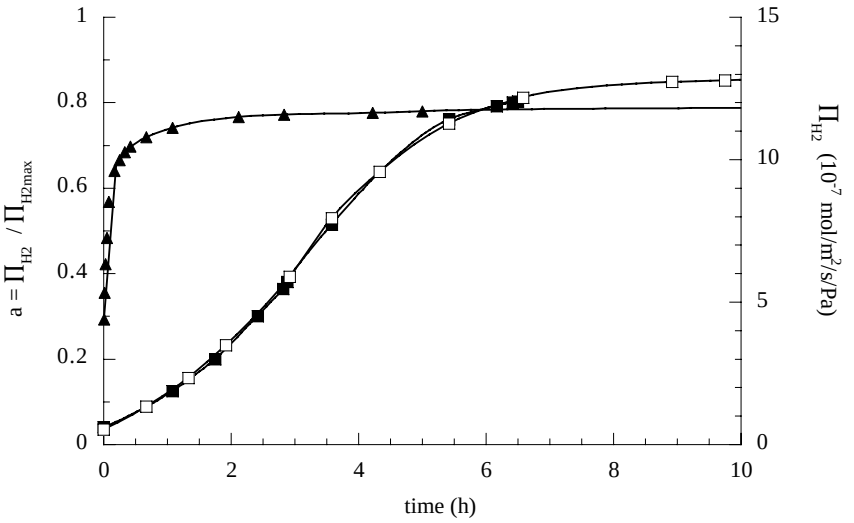

Fig. 5. Comparison of water (▲) and *n*-butane (□/■) desorption curves of the lower quality membrane E. Please note the absolute permeance axis on the right.

This trend, even more pronounced, was also observed on the higher quality membrane B as can be seen in Fig. 6. Therefore, it is difficult to use water desorption to differentiate between high a low quality membranes.

4.4. Maximum values of desorbed amounts of water and n-butane

The residual amounts of water and *n*-butane after desorption may reflect the adsorption force between

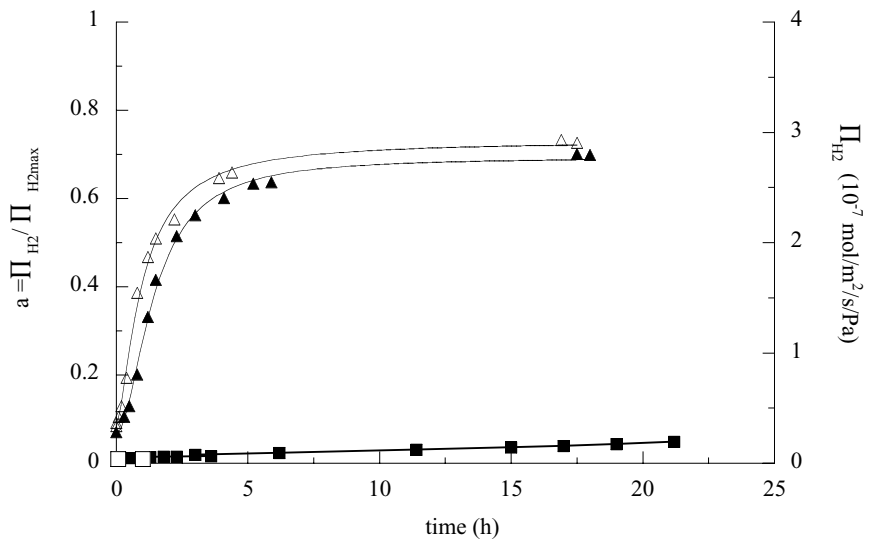

Fig. 6. Comparison of water (▲/△) and *n*-butane (□/■) desorption curves of the higher quality membrane B. Please note the absolute permeance axis on the right.

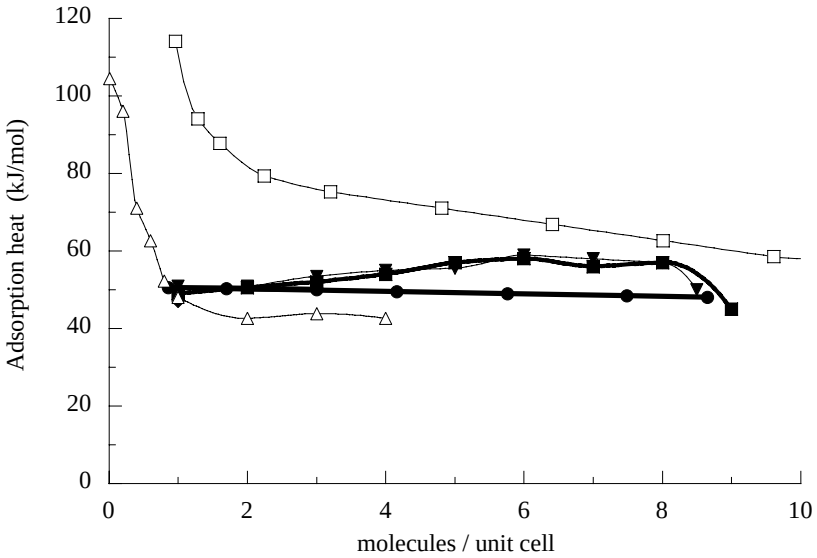

Fig. 7. Adsorption heats of water and *n*-butane in ZSM-5 with different Si/Al ratio from literature data: *n*-butane (■) on silicalite [33]; (▼) on ZSM-5 with Si/Al = 132 [35]; (●) on silicalite [23]; water (□) on ZSM-5 with Si/Al = 37 [36]; (△) on silicalite [37].

the molecules and membrane surface. Fig. 7 shows literature data on water and *n*-butane adsorption heats of ZSM-5 zeolite with different ratio of Si/Al and different surface coverage. The adsorption heats of water and *n*-butane are comparable at high coverage (ca. 60 kJ/mol for both), whereas, at low coverage water adsorption heats are significantly higher (120 kJ/mol) than for *n*-butane (60 kJ/mol) (see Fig. 7). It indicates that a complete desorption of water from ZSM-5 zeolite is more difficult than for *n*-butane. This is in agreement with our experimental findings. The maximum values of hydrogen permeance through the wet membranes were systematically lower (about 70% of the dry membrane value) when compared to those obtained with *n*-butane (90%), on lower quality membranes, after 23 h.

5. Conclusion

The low diffusion coefficient of *n*-butane together with its relatively high adsorption heat in ZSM-5 microporous system, make this molecule an efficient probe to study zeolite membrane quality, using the described dynamic desorption procedure. This simple quality test is based on the measurement of the permeation of a non-adsorbed gas through a membrane saturated by an adsorbing molecule, as *n*-butane.

Nevertheless, this adsorbing molecule should not have too high a diffusion coefficient, in order to avoid a fast and therefore indiscriminating desorption.

In comparison with the sophisticated equipment necessary to characterise the membrane by separation tests, this work present a simple, still effective, approach, that could be used in the future as a quality control for industrial production of zeolite membranes. As a matter of fact, the laboratory procedures used here for thorough studies (well-defined gases, long-term experiments) can be easily simplified to be adapted to an industrial quality control process.

Acknowledgements

This investigation was supported by the Grant Agency of the Czech Republic as Grant No. 104/01/0945 and by the Grant Agency of the Academy of Sciences of the Czech Republic as the Grant No. A 1040101. The French Région Rhône-Alpes PECO program is also acknowledged. Drs. J. Rathousky and A. Zukal, from the Academy of Sciences of the Czech Republic are also kindly acknowledged for

the data they provided on *n*-butane adsorption in MCM-41.

References

[1] I. Kumakiri, T. Yamaguchi, S.-i. Nakao, Preparation of zeolite A and faujasite membranes from a clear solution, Ind. Eng. Chem. Res. 38 (1999) 4682.

[2] K. Jansen, T. Mashmeyer, Progress in zeolitic membranes, Topics Catal. 9 (1999) 113.

[3] K.C. Jansen, E.N. Coker, Zeolitic membranes, Curr. Opin. Solid State Mater. Sci. 1 (1996) 65.

[4] C. Chau, I. Prévost, S. Miachon, J.-A. Dalmon, Procédé de préparation de membrane zéolithique supportée par cristallisation contrôlée en température, European Patent 02290252.2-2113 (4 February 2001).

[5] G. Li, E. Kikuchi, M. Matsukata, ZSM-5 zeolite membranes prepared from a clear template-free solution, Microporous Mesoporous Mater. 60 (2003) 225.

[6] A. Giroir-Fendler, J. Peureux, H. Mozzanega, J.-A. Dalmon, Characterisation of a zeolite membrane for catalytic membrane reactor application, St. Surf. Sci. Catal. 101A (1996) 127.

[7] Y. Takata, T. Tsuru, T. Yoshioka, M. Asaeda, Gas permeation properties of MFI zeolite membranes prepared by the secondary growth of colloidal silicalite and application to the methylation of toluene, Microporous Mesoporous Mater. 54 (2002) 257.

[8] M. Noack, P. Kölsch, R. Schäfer, P. Toussaint, J. Caro, Molecular sieve membranes for industrial application: problems, progress, solutions, Chem. Eng. Technol. 25 (2002) 221.

[9] S.M. Lai, L.T.Y. Au, K.L. Yeung, Influence of the synthesis conditions and growth environment on MFI zeolite film orientation, Microporous Mesoporous Mater. 54 (2002) 63.

[10] E. Piera, C.A.M. Brenninkmeijer, J. Santamaría, J. Coronas, Separation of traces of CO from air using MFI-type zeolite membranes, J. Membr. Sci. 201 (2002) 229.

[11] J. Hedlund, J. Sterte, M. Anthonis, A.-J. Bons, B. Carstensen, N. Corcoran, D. Cox, H. Deckman, W.D. Gijnst, P.-P.d. Moor, F. Lai, J. McHenry, W. Mortier, J. Reinoso, J. Peters, High-flux MFI membranes, Microporous Mesoporous Mater. 52 (2002) 179.

[12] T.Q. Gardner, J.L. Falconer, R.D. Noble, Adsorption and diffusion properties of zeolite membranes by transient permeation, J. Membr. Sci. 149 (2002) 435.

[13] M. Nomura, T. Yamaguchi, S.-i. Nakao, Transport phenomena through intercrystalline and intracrystalline pathways of silicalite zeolite membranes, J. Membr. Sci. 187 (2001) 203.

[14] J. Dong, Y.S. Lin, M.Z.-C. Hu, R.A. Peascoe, E.A. Payzant, Template-removal-associated microstructural development of porous-ceramic-supported MFI zeolite membranes, Microporous Mesoporous Mater. 34 (2000) 241.

[15] P. Ciavarella, H. Moueddeb, S. Miachon, K. Fiatty, J.-A. Dalmon, Experimental study and numerical simulation of hydrogen/isobutane permeation and separation using MFI-zeolite membrane reactor, Catal. Today 56 (2000) 253.

[16] C. Bai, M. Jia, J. Falconer, R.D. Noble, Preparation and separation properties of silicalite composite membranes, J. Membr. Sci. 105 (1995) 79.

[17] F. Kapteijn, W.J.W. Bakker, J.v.d. Graaf, G. Zheng, J. Poppe, J.A. Moulijn, Permeation and separation behavior of a silicalite-1 membrane, Catal. Today 25 (1995) 213.

[18] Z.A.E.P. Vroon, K. Keizer, A.J. Burggraaf, H. Verweij, Preparation and characterization of thin zeolite MFI membranes on porous supports, J. Membr. Sci. 144 (1998) 65.

[19] S.-i. Nakao, Determination of pore size distribution. 3. Filtration membranes, J. Membr. Sci. 96 (1994) 131.

[20] T. Tsuru, T. Hino, T. Yoshioka, M. Asaeda, Permporometry characterization of microporous ceramic membranes, J. Membr. Sci. 186 (2001) 257.

[21] M. Jiang, M. Eic, S. Miachon, J.-A. Dalmon, M. Kocirik, Diffusion of *n*-butane, isobutane and ethane in a MFI-zeolite membrane investigated by gas permeation and ZLC measurements, Sep. Purification Technol. 25 (2001) 287.

[22] T.J.H. Vlugt, Adsorption and diffusion in zeolites: a computational study, Ph.D. thesis, University of Amsterdam, Amsterdam, 2000.

[23] M.S. Sun, D.B. Shah, H. Xu, O. Talu, Adsorption equilibria of C1 to C4 alkanes, CO_2, and SF_6 on silicalite, J. Phys. Chem. 102 (1998) 1466.

[24] J. Rathousky, A. Zukal, unpublished data, 2002.

[25] R.M. Barrer, J.A. Lee, Sorption isotherms and enthalpies, Surf. Sci. 12 (1968) 341.

[26] J.P.V.d. Berg, J.P. Wolthuizen, A.D.H. Clague, G.R. Hays, R. Huis, J.H.C.v. Hoof, Low-temperature oligomerization of small olefins on zeolite H-ZSM-5. An investigation with high-resolution solid-state carbon-13 NMR, J. Catal. 80 (1983) 130.

[27] J.P.V.d. Berg, J.P. Wolthuizen, J.H.C.v. Hoof, Reaction of small olefins on zeolite H-ZSM-5. A thermogravimetric study at low and intermediate temperatures, J. Catal. 80 (1983) 139.

[28] J.P. Wolthuizen, J.P.V.d. Berg, J.H.C.v. Hoof, Low temperature reactions of olefins on partially hydrated zeolite H-ZSM-5, Stud. Surf. Sci. Catal. 5 (1980) 85.

[29] A. Zikanova, M. Kocirik, M. Derewinski, P. Sarv, J. Dubsky, P. Hudec, A. Smieskova, Immobilization and mobilization of surface species during transformation of ethylene over HZSM-5, Stud. Surf. Sci. Catal. 135 (2001) 24.

[30] I. Kumakiri, S. Miachon, J.-A. Dalmon, Zeolite membrane application to ammonia separation, in preparation.

[31] C. Bussai, S. Hannongbua, S. Fritzsche, R. Haberlant, Ab initio potential energy surface and molecular dynamics simulations for the determination of the diffusion coefficient of water in silicalite-1, Chem. Phys. Lett. 354 (2002) 310.

[32] J. Caro, S. Hocevar, J. Karger, L. Riekert, Intracrystalline self-diffusion of water and methane in ZSM-5 zeolites, Zeolites 6 (1986) 213.

[33] D. Shen, L.V. Rees, Adsorption and diffusion of *n*-butane and 2-butyne in silicalite I, Zeolites 11 (1991) 684.

[34] K.P. Datema, C.J.J.D. Ouden, W.D. Ylstra, H.P.C.E. Kuipers, M.F.M. Post, J. Kaerger, Fourier-transform pulsed-field-gradient proton nuclear magnetic resonance investigation of the diffusion of light *n*-alkanes in zeolite ZSM-5, J. Chem. Soc., Faraday Trans. 87 (1991) 1935.

[35] R.E. Richards, L.V.C. Rees, Sorption and packing of *n*-alkane molecules in ZSM-5, Langmuir 3 (1987) 335.

[36] D.H. Olson, W.O. Haag, W.S. Borghard, Use of water as a probe of zeolitic properties: interaction of water with HZSM-5, Microporous Mesoporous Mater. 35-36 (2000) 435.

[37] F. Vigne-Maeder, A. Auroux, Potential maps of methane, water, and methanol in silicalite, J. Phys. Chem. 94 (1990) 316.